J Fluoresc (2011) 21:1847–1856
DOI 10.1007/s10895-011-0879-2

ORIGINAL PAPER

Spectroscopic Investigation on the Synergistic Effects of Ultrasound and Dioxopromethazine Hydrochloride on Protein

Ling-Ling He · Xin Wang · Bin Liu · Jun Wang · Ya-Guang Sun · Shu-Kun Xu

Received: 19 October 2010 / Accepted: 13 February 2011 / Published online: 22 March 2011

Abstract The bovine serum albumin (BSA) was selected as a target molecule, the sonodynamic damage to protein in the presence of dioxopromethazine hydrochloride (DPZ) and its mechanism were studied by means of absorption and fluorescence spectra. The results of hyperchromic effect of absorption spectra and quenching of intrinsic fluorescence spectra indicated that the synergistic effects of ultrasound and DPZ could induce the damage of BSA molecules. The damage degree of BSA molecules increased with the increase of ultrasonic irradiation time and DPZ concentration. The results of synchronous fluorescence and three-dimensional fluorescence spectra further confirmed that the synergistic effects of ultrasound and DPZ induced the damage of BSA molecules. The results of oxidation-extraction photometry with several reactive oxygen species (ROS) scavengers indicated that the damage of BSA molecules could be mainly due to the generation of ROS, in which both $^1O_2$ and ·OH were the important mediators of the ultrasound-inducing BSA molecules damage in the presence of DPZ.

L.-L. He · B. Liu · S.-K. Xu (✉)
Department of Chemistry, Northeastern University,
Shenyang 110819, People's Republic of China
e-mail: xushukun46@126.com

L.-L. He · Y.-G. Sun
College of Applied Chemistry,
Shenyang University of Chemical Technology,
Shenyang 110142, People's Republic of China

X. Wang · B. Liu
School of Pharmaceutical Sciences, Liaoning University,
Shenyang 110036, People's Republic of China

J. Wang
Department of Chemistry, Liaoning University,
Shenyang 110036, People's Republic of China

Keywords Spectroscopy · Ultrasound · Dioxopromethazine hydrochloride · Protein damage · Reactive oxygen species

Introduction

Photodynamic therapy (PDT) is a useful technique for the treatment of cancer. In the presence of oxygen, the photosensitizer can be activated by visible light of appropriate wavelength and generate reactive oxygen species (ROS) which can cause the apoptosis and/or necrosis of tumor cells [1, 2]. At present, PDT is being tested in the clinic for use in oncology to treat various cancers [3–9]. Although PDT has given encouraging results in clinical trials, it has a major problem. PDT can be applied only to the superficial lesions of tissues because of the limited penetration of light into tumor tissue [10]. In recent years, a promising new modality for treating cancer called sonodynamic therapy (SDT), in which the activation of sonosensitizers is carried out using ultrasound irradiation, has been introduced to overcome the minimal tissue penetrating ability of light in PDT [11, 12]. Ultrasound has an appropriate tissue attenuation coefficient for penetrating intervening tissues to reach non-superficial objects while maintaining the ability to focus energy into small volumes [13, 14].

Recently, SDT has been widely investigated focusing on the mechanisms of killing effects by using different ultrasound parameters and different sonosensitizers [15, 16]. Most of them regarded the tumor cells as assault target, and achieved the goal of treating tumors through damaging cell membrane [16]. The damage to intracellular substances might be a more effective method to kill the tumor cells. If the proteins in the tumor cells were damaged by sonosensitive drug under ultrasonic irradiation, the whole cells would undergo apoptosis abnormally [17].

Dioxopromethazine hydrochloride (DPZ) is chemically named as 5,5-Dioxo-10-(2-(dimethylamino) propyl) phenothiazine hydrochloride (Fig. 1). It is one of the most important compounds of the phenothiazine derivatives and has the functions of preventing cough, antihistamine, relieving the spasm of smooth muscle, anti-inflammation and local anesthesia. It has been widely used to cure acute or chronic bronchitis, rhinitis, cough, nettle rash and pruritus in clinic [18, 19]. In addition, many phenothiazine derivatives have been investigated and used as biological photosensitizers of photodynamic therapy (PDT) [20–22]. Many photosensitizers can be used as sonosensitizers in the research of SDT [23–25], which demonstrate that phenothiazine derivatives have potential to be used as sonochemical sensitizer for tumor treatment in combination with ultrasound. However, the sonodynamic activity of DPZ and its mechanism have not been reported.

Reactive oxygen species (ROS) are a class of ubiquitous molecules such as superoxide anion radical ($\cdot O_2$-), hydrogen peroxide (H_2O_2), hydroxyl radical ($\cdot OH$), and singlet oxygen ($^1O_2$) and have been implicated in many biological processes [26]. Lots of reports indicate that ROS play a primary role in ultrasonically induced apoptosis of cells in the presence of sonosensitizer [10, 27–29] and many technologies and methods, such as electron spin resonance [30, 31], chemiluminesce [32], oxidation-extraction photometry [33], free radical scavengers [34, 35], etc., have been used in the study on the generation and kind of ROS in SDT.

In this work, the bovine serum albumin (BSA) was selected as a target molecule, the sonodynamic damage to protein in the presence of DPZ and its mechanism were studied by means of absorption and fluorescence spectra. Firstly, sonodynamic damage of BSA in the presence of DPZ was investigated. Some influencing factors, such as ultrasonic irradiation time and DPZ concentration, were also studied systemically. Secondly, the mechanism of synergistic effects of ultrasound and DPZ was investigated by means of oxidation-extraction photometry with several ROS scavengers. It is expected that this report would offer some valuable references to use DPZ or its derivatives as sonosensitive drug to treat tumor in the future.

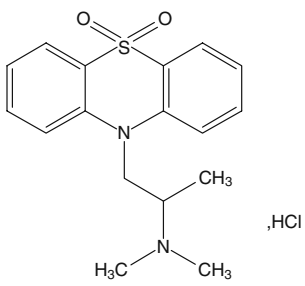

Fig. 1 Molecular structure of DPZ

Experimental Section

Materials

BSA (Fraction V) was obtained from Amresco (USA) and used without further purification. DPZ was obtained from the Liaoning Donggang Hongda Pharmaceutical Co., Ltd. (China). The BSA stock solution, 5.00×10^{-5} mol L^{-1}, was prepared in 0.05 mol L^{-1} Tris-HCl buffer solution of pH 7.40 containing 0.05 mol L^{-1} NaCl, then stored at 0−4 °C in the refrigerator. The DPZ stock solution, 5.00×10^{-5} mol L^{-1}, was prepared in the same buffer solution. All the other materials were of analytical reagent grade and used without further purification. Doubly distilled water was used to prepare solutions.

Apparatus

The fluorescence spectra were carried out on an LS-55 fluorescence spectrophotometer (Perkin-Elmer, USA). Fluorescence spectra were obtained at an excitation wavelength of 285 nm, with the slit widths of both the excitation and emission set at 2.5 nm and the scanning speed of 1,200 nm min^{-1}. The synchronous fluorescence spectra were obtained by simultaneously scanning excitation and emission monochromators. As $\Delta\lambda$ between excitation wavelength and emission wavelength is 15 nm, synchronous fluorescence offers characteristics of Tyr residues, while $\Delta\lambda$ is 60 nm, it provides the characteristic information of Trp residues [36]. The three-dimensional fluorescence spectra were performed under the following conditions: the initial excitation wavelength at 200 nm, the emission wavelength between 200 nm and 800 nm, scanning number 30 and increment 5 nm with other parameters just as the same to those of the fluorescence spectra. The absorption spectra were recorded on a UV-1201 spectrophotometer (Beijing Rayleigh Analytical Instrument Co., Ltd., China) in the range of 200–400 nm with the slit width set at 1 nm. The controllable serial-ultrasonics apparatus (KQ5200DB, Kunshan Ultrasonic Instruments Co., Ltd., China) shown in Fig. 2 was used as irradiation source, operating at ultrasonic frequency of 40 kHz and output power of 200 W through manual adjusting. All pH measurements were made with a pHS-25 digital pH-meter (Shanghai Reaches Instrument Co., Ltd., China).

Procedures

The experiments of sonodynamic damage of BSA under ultrasonic irradiation with and without DPZ were performed according to the method of Wang et al. [37] with some modification. Firstly, four 25.00 mL volumetric flasks were marked with a–d, respectively. Four 5.00 mL BSA stock solution were taken and put into volumetric flasks a–

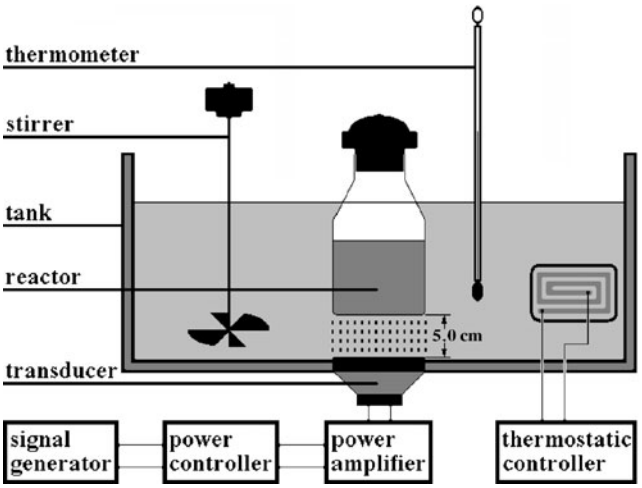

Fig. 2 The apparatus of ultrasonic irradiation

d, respectively. Then, two 5.00 mL of DPZ stock solution were added into volumetric flasks b and d, respectively. Finally, all volumetric flasks were diluted to 25.00 mL with Tris-HCl-NaCl solutions. The final concentration of BSA and DPZ were both of 1.00×10^{-5} mol L^{-1}. The solutions a and b were put into an ultrasonic apparatus away from light directly under ultrasonic irradiation, while the solutions c to d were only placed away from light without ultrasonic irradiation. After 3.0 h, the absorption and fluorescence spectra of each sample solution were determined to evaluate the damage of BSA molecules. In addition, the effects of ultrasonic irradiation time and DPZ concentration on the damage of BSA were also examined.

The oxidation-extraction photometry method is an effective method to determine ROS with many advantages, such as fast and accurate detection, simple equipment requirements, low-cost reagent, wide detection range and simple requirements for sample, etc. [38]. In this method, 1,5-diphenylcarbohydrazide (DPCI) can be oxidized by ROS into diphenylcarbonzone (DPCO), which can be extracted by organic solvents and shows the maximum absorption at 563 nm. The absorbance values of DPCO at 563 nm are correlated to the quantities of ROS generation. The experiments to confirm the generation of ROS were performed according to the method of Liu et al. [33] with some modification. Firstly, the effects of DPZ concentration on the generation of ROS were examined. In six 50.00 mL volumetric flasks, the final concentration of DPCI were both 5.00×10^{-3} mol L^{-1}, and the final concentration of DPZ were changed from 0.00 mol L^{-1} to 2.50 mol L^{-1} at 0.50 mol L^{-1} intervals. Then, each of them (25.00 mL) was transferred into 50 mL conical flask and placed in an ultrasonic irradiation apparatus, the other (25.00 mL) was kept in the dark. After 3.0 h, the solutions (10.00 mL) were extracted repeatedly with Benzene-CCl_4 (1:1) mixed solution. The extraction solutions were diluted to 10.00 mL with the extractant and detected at 563 nm by absorption spectrophotometer. Secondly, the effects of ultrasonic irradiation time on the generation of ROS were examined. The final concentration of DPCI and DPZ were 5.00×10^{-3} mol L^{-1} and 2.00×10^{-4} mol L^{-1}, respectively. The ultrasonic irradiation time were changed from 1.0 h to 6.0 h at 1.0 h intervals. Thirdly, to confirm the kind of ROS inducing BSA damage, several scavengers, such as sodium azide (NaN_3), dimethyl sulfoxide (DMSO), L-histidine (L-His), ascorbic acid (V_C), were used to quench different ROS. The final concentration of DPCI and DPZ were 5.00×10^{-3} mol L^{-1} and 2.00×10^{-4} mol L^{-1}, respectively. All of the quencher's concentrations were 5.00×10^{-2} mol L^{-1}.

Results and Discussion

Absorption and Fluorescence Spectra of BSA and BSA-DPZ Mixed Solutions With and Without Under Ultrasonic Irradiation

The absorption and fluorescence spectra of BSA and BSA-DPZ mixed solutions at different conditions are shown in Fig. 3. It can be seen from Fig. 3a that the BSA solution has

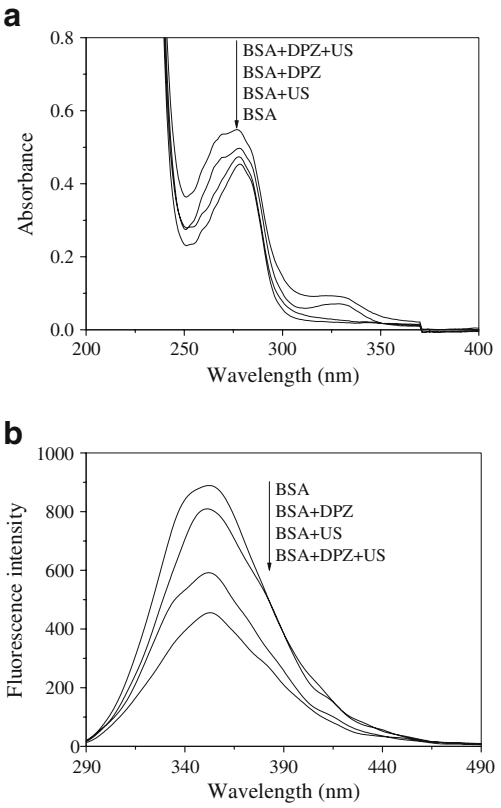

Fig. 3 Absorption spectra (**a**) and fluorescence spectra (**b**) of BSA and BSA-DPZ mixed solutions at different conditions, [BSA] = 1.00×10^{-5} mol L^{-1}, [DPZ] = 1.00×10^{-5} mol L^{-1}, t_{US} = 3.0 h, US: ultrasound

a strong absorption peak at 278 nm. When BSA mixed with DPZ, the maximum absorption wavelength emerges blue shift to 277 nm and the absorbance intensity increases obviously, which indicates that there is an interaction between DPZ and BSA and forms one protein—drug complex with certain new structure [18]. After ultrasonic irradiation for 3.0 h, the BSA and BSA-DPZ mixed solutions both show hyperchromic effects compared with corresponding those without ultrasonic irradiation. In addition, the BSA-DPZ mixed solution exhibit more obvious hyperchromic effect than pure BSA solution. These results can be explained that water can generate some ROS due to the cavitations effect of ultrasonic irradiation [39] and induce the damage of BSA molecules. Moreover, DPZ can be activated by ultrasound and undergo effective energy transfer to generate more ROS. And because of the binding of DPZ to BSA, the very short distance makes ROS induce the damage to BSA molecules more effective.

As shown in Fig. 3b, it is obvious that BSA has a strong fluorescence emission peaked at 350.5 nm after being excited with the wavelength of 285 nm. The fluorescence of BSA is quenched by DPZ due to the interaction between DPZ and BSA and a non-fluorescent complex is formed [18]. Under ultrasonic irradiation, the fluorescence intensities of BSA and BSA-DPZ mixed solutions decrease obviously. And the fluorescence intensity of BSA-DPZ mixed solution decreases more strikingly. The intrinsic fluorescence of proteins comes from phenylalanine (Phe), tyrosine (Tyr) and tryptophan (Trp) residues although they

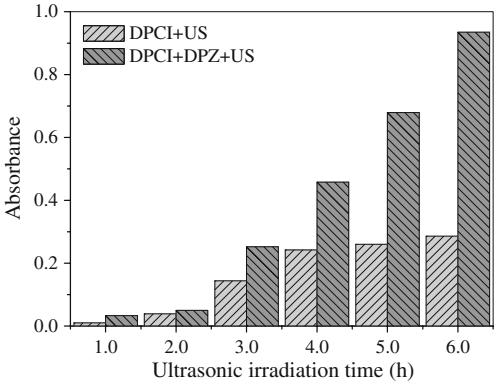

Fig. 5 Changes of absorbance of DPCO at 563 nm in the DPCI and DPCI-DPZ mixed solutions with different ultrasonic irradiation time, [DPCI] = 5.00×10^{-3} mol L^{-1}, [DPZ] = 2.00×10^{-4} mol L^{-1}

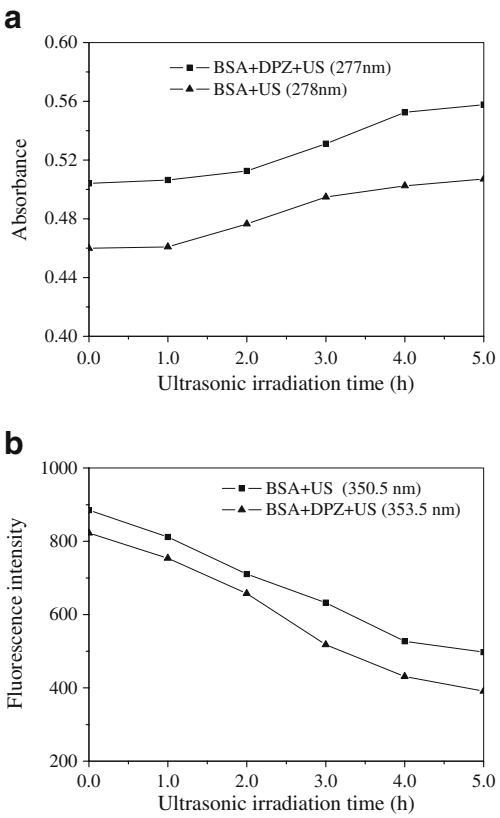

Fig. 4 Changes of absorbance (**a**) and fluorescence intensity (**b**) of BSA and BSA-DPZ mixed solutions with different ultrasonic irradiation time, [BSA] = 1.00×10^{-5} mol L^{-1}, [DPZ] = 1.00×10^{-5} mol L^{-1}

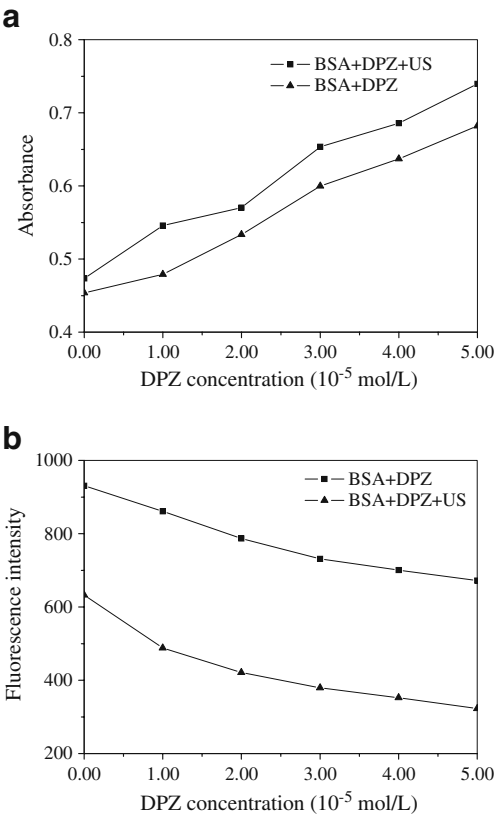

Fig. 6 Changes of absorbance (**a**) and fluorescence intensity (**b**) of BSA-DPZ mixed solutions with different DPZ concentration, [BSA] = 1.00×10^{-5} mol L^{-1}, t_{US} = 3.0 h

are relatively rare in proteins [40]. The fluorescence of Phe residue usually can be negligible. Under ultrasonic irradiation, the generated ROS induce the oxidation of Trp and Tyr residues and the fluorescence of them are quenched. Furthermore, the synergistic effects of ultrasound and DPZ induce more serious damage to BSA molecules. These results coincide with those obtained from the absorption spectra above.

Effect of Ultrasonic Irradiation Time on Damage of BSA

The effect of ultrasonic irradiation time on the damage of BSA was investigated by changes of absorbance and fluorescence intensities. As shown in Fig. 4a, the absorbance increase with the increase of ultrasonic irradiation time whether in the presence or absence of DPZ. Moreover, the absorbance of BSA-DPZ mixed solution is much higher than corresponding that of BSA solution at any ultrasonic irradiation time. The corresponding results of fluorescence intensity changes are shown in Fig. 4b. It can be seen that the fluorescence intensities decrease with the increase of ultrasonic irradiation time, and the fluorescence intensities of BSA-DPZ mixed solution are obviously lower than those of BSA solution at any ultrasonic irradiation time. These results indicate that the degree of BSA molecules damage enhance with the increasing ultrasonic irradiation time. Moreover, the synergistic effects of ultrasound and DPZ induce more serious damage to BSA molecules. It can be inferred that the quantities of generated ROS in the solutions also increase gradually with the increase of ultrasonic irradiation time.

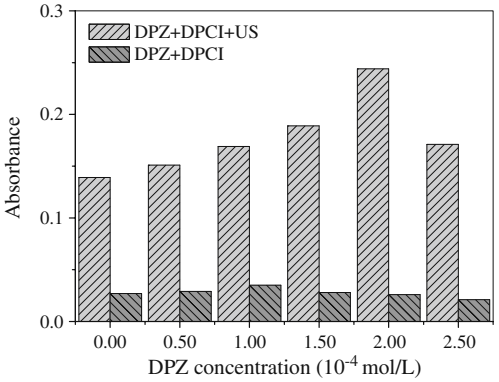

Fig. 8 Changes of absorbance of DPCO at 563 nm in the DPCI-DPZ mixed solutions with different DPZ concentration, [DPCI] = 5.00×10^{-3} mol L^{-1}, t_{US} = 3.0 h

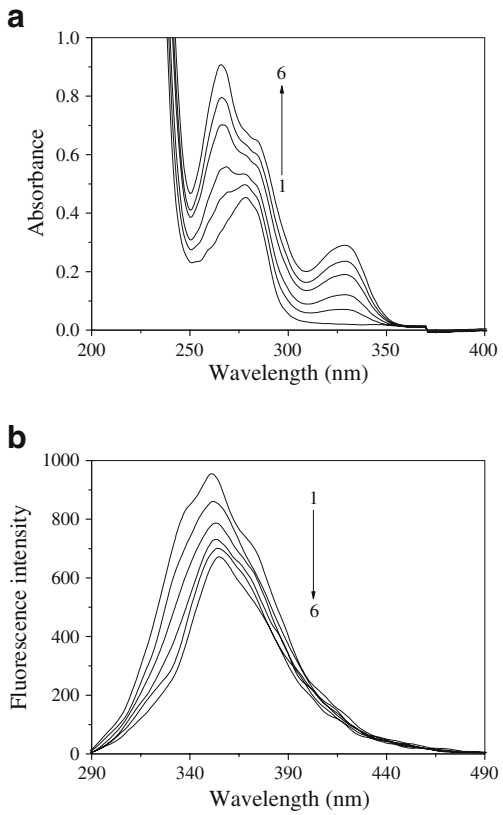

Fig. 7 Absorption spectra (**a**) and fluorescence quenching spectra (**b**) of BSA in the presence of different concentrations of DPZ, [BSA] = 1.0×10^{-5} mol L^{-1}; [DPZ] (1–6): 0, 1.0, 2.0, 3.0, 4.0, 5.0×10^{-5} mol L^{-1}

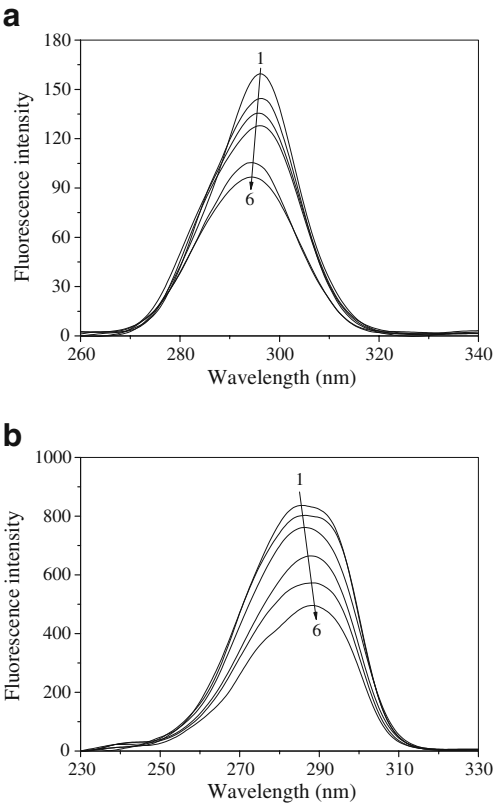

Fig. 9 Synchronous fluorescence spectra of BSA solutions with different ultrasonic irradiation time at Δλ = 15 nm (**a**) and Δλ = 60 nm (**b**), [BSA] = 1.00×10^{-5} mol L^{-1}, t_{US} (1–6) = 0, 1.0, 2.0, 3.0, 4.0, 5.0 h

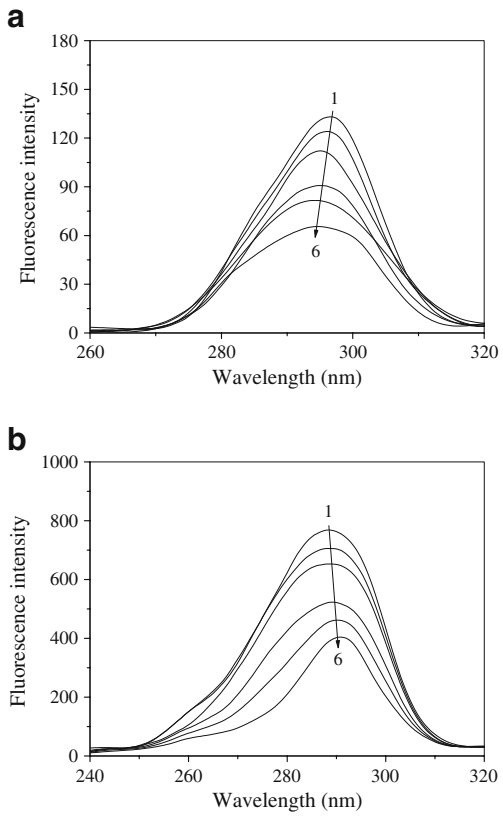

Fig. 10 Synchronous fluorescence spectra of BSA-DPZ mixed solutions with different ultrasonic irradiation time at $\Delta\lambda$ = 15 nm (**a**) and $\Delta\lambda$ = 60 nm (**b**), [BSA] = 1.00×10^{-5} mol L^{-1}, [DPZ] = 1.00×10^{-5} mol L^{-1}, t_{US} (1–6) = 0, 1.0, 2.0, 3.0, 4.0, 5.0 h

In order to confirm the preliminary inferences, the oxidation-extraction photometry method was used to determine the generated ROS in solutions under ultrasonic irradiation. The absorbance values of DPCO showed in Fig. 5 are the absorbance difference values of solutions under ultrasonic irradiation and kept in the dark. It can be seen that the absorbance of DPCO at 563 nm both increase with the increase of ultrasonic irradiation time in the presence and absence of DPZ. However, the absorbance of DPCO in DPCI-DPZ mixed solution is much higher than corresponding that in the DPCI solution at any ultrasonic irradiation time. And the difference values of absorbance of them increase with the increasing ultrasonic irradiation time. These results indicate that the ability of ROS generation is very limited for simple ultrasonic irradiation. Moreover, DPZ can be activated by ultrasound and generate ROS more effectively, and the quantities of ROS increase with the increase of ultrasonic irradiation time. Therefore, the damage of BSA becomes increasingly serious.

Effect of DPZ Concentration on Damage of BSA

The changes of absorbance and fluorescence intensity of BSA-DPZ mixed solutions with different DPZ concentration are shown in Fig. 6. Because of the interaction between DPZ and BSA, the maximum absorption wavelength of BSA emerges blue shift from 278 nm to 266 nm and the maximum fluorescence emission wavelength emerges red shift from 350.5 nm to 354.5 nm (Fig. 7). It can be seen from Fig. 6a that with the increase of DPZ concentration, the absorbance at the maximum absorption wavelength of BSA in BSA-DPZ mixed solution increase gradually with and without ultrasonic irradiation. Moreover, the hyperchromic effect under ultrasonic irradiation is higher than that without ultrasonic irradiation. These results indicate that more chromophoric amino acid residues are exposed with the increase of DPZ concentration gradually. And then, BSA molecules are damaged sequentially and the peptide chain spread much more under ultrasonic irradiation. The corresponding results of fluorescence intensity changes are shown in Fig. 6b. It can be seen that the fluorescence intensities of maximum fluorescence emission wavelength of BSA-DPZ mixed solutions decrease with the increase of DPZ concentration with and without the ultrasonic irradiation. After being irradiated by ultrasound, the fluorescence intensity of BSA-DPZ mixed solutions decrease much faster compared with that without ultrasonic irradiation. It can be inferred that the quantity of ROS generation in unit time in the solutions also increase and the oxidation possibilities of BSA molecules also become higher with the increase of DPZ concentration.

From Fig. 8 it can be seen that the absorbance of DPCO at 563 nm of DPCI-DPZ mixed solution kept in the dark have no obvious change with the increase of DPZ concentration. However, under ultrasonic irradiation, the absorbance of DPCO at 563 nm of DPCI-DPZ mixed

Table 1 Synchronous fluorescence quenching ratios (R_{FQ}) of BSA and BSA-DPZ mixed solutions with different ultrasonic irradiation time

t_{US} (h)		0	1.0	2.0	3.0	4.0	5.0
$\Delta\lambda$ = 15	BSA	0	9.42	15.01	19.79	33.86	39.41
	BSA-DPZ	16.53	22.29	29.66	43.06	48.81	58.92
$\Delta\lambda$ = 60	BSA	0	4.01	8.95	20.54	31.52	40.69
	BSA-DPZ	8.13	15.62	21.94	37.46	44.77	51.68

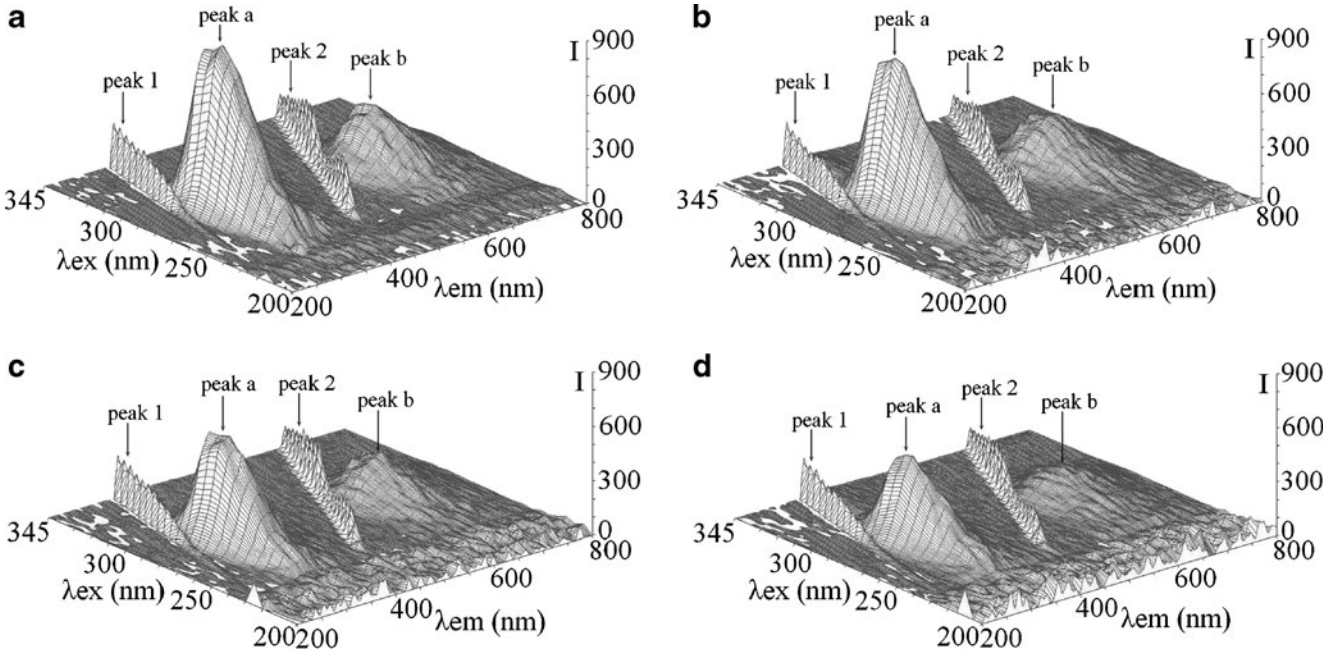

Fig. 11 Three-dimensional fluorescence spectra of BSA (**a**), BSA-DPZ (**b**), BSA + US (**c**), BSA-DPZ + US (**d**), [BSA] = [DPZ] =1.00×10^{-5} mol/L, t_{US} = 3.0 h

solution increase significantly with the increasing DPZ concentration when DPZ concentration is less than 2.00×10^{-4} mol L^{-1}. The results indicate that the quantity of ROS generation increase with the increase of DPZ concentration under ultrasonic irradiation. In addition, the absorbance of DPCO of DPCI-DPZ mixed solution at 563 nm decreases when DPZ concentration is more than 2.00×10^{-4} mol L^{-1} under ultrasonic irradiation. The reason might be that the high DPZ concentration would inhibit the light transmission from sonoluminescence.

Synchronous Fluorescence Spectra of BSA and BSA-DPZ Solutions with Different Ultrasonic Irradiation Time

Synchronous fluorescence measurements provide information about the molecular microenvironment in the vicinity

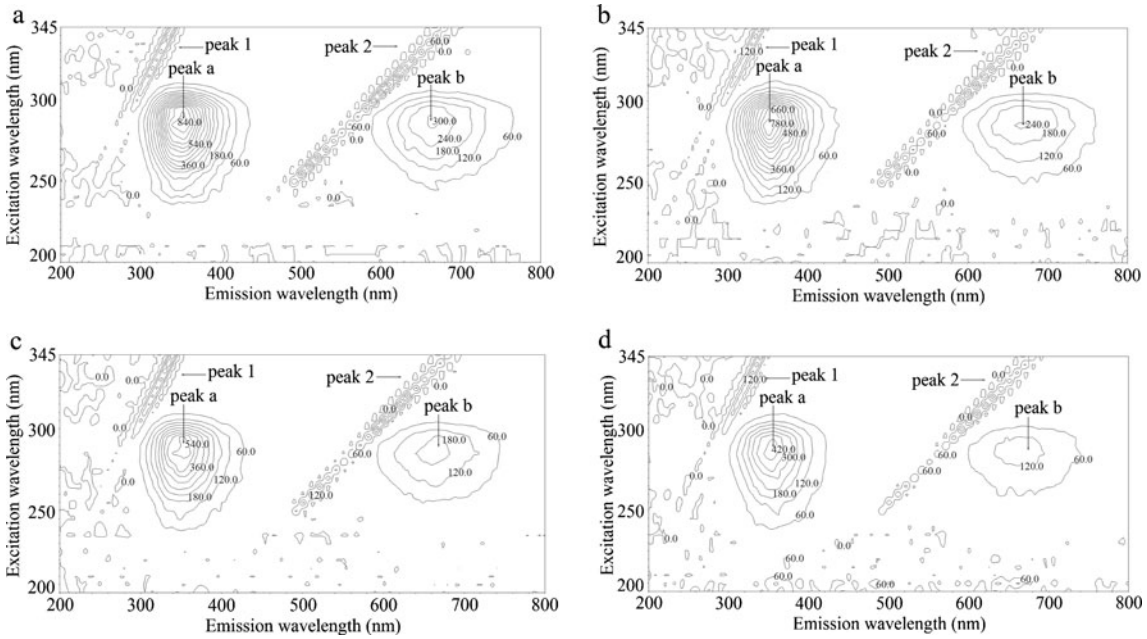

Fig. 12 Contour spectra of BSA (**a**), BSA-DPZ (**b**), BSA + US (**c**), and BSA-DPZ + US (**d**), [BSA] = [DPZ] = 1.00×10^{-5} mol/L, t_{US} = 3.0 h

Table 2 Three-dimensional fluorescence spectral characteristics of BSA, BSA-DPZ, BSA + US, and BSA-DPZ + US

Systems and parameters		Peak a	Peak b
BSA	Peak position $\lambda_{ex}/\lambda_{em}$ nm/nm)	285.0/350.5	285.0/666.0
	Fluorescence intensity	896.6	313.6
	Stokes $\Delta\lambda$ (nm)	65.5	381.0
BSA-DPZ	Peak position $\lambda_{ex}/\lambda_{em}$ (nm/nm)	285.0/352.5	285.0/665.5
	Fluorescence intensity	817.2	245.3
	Stokes $\Delta\lambda$ (nm)	67.5	380.5
BSA + US	Peak position $\lambda_{ex}/\lambda_{em}$ (nm/nm)	285.0/350.0	285.0/667.0
	Fluorescence intensity	604.9	222.4
	Stokes $\Delta\lambda$ (nm)	65.0	382
BSA-DPZ + US	Peak position $\lambda_{ex}/\lambda_{em}$ (nm/nm)	285.0/353.5	285.0/660.0
	Fluorescence intensity	464.7	151.8
	Stokes $\Delta\lambda$ (nm)	68.5	375.0

of the fluorescent functional groups [41]. The synchronous fluorescence spectra of BSA solutions in the absence and presence of DPZ with the increase of ultrasonic irradiation time are shown in Figs. 9 and 10. It can be seen that the fluorescence intensities of Tyr and Trp residues both decrease with the increase of ultrasonic irradiation time. Meanwhile, the maximum emission wavelengths of Tyr residues shift towards short wavelength with the increase of ultrasonic irradiation time, which indicates that Tyr residues are located in a more hydrophobic environment and less exposed to the solvent. On the contrary, the maximum emission wavelengths of Trp residues shift towards long wavelength with the increase of ultrasonic irradiation time, which indicates that Trp residues are located in a more polar environment and more exposed to the solvent [42]. In addition, the synchronous fluorescence quenching ratios (R_{FQ}) were calculated by using the equation $R_{FQ}(\%) = (1 - F/F_0) \times 100$, where F_0 represents the synchronous fluorescence intensity of BSA solution without ultrasonic irradiation, and F represents the synchronous fluorescence intensity of BSA or BSA-DPZ mixed solution with different ultrasonic irradiation time. From Table 1 it can be seen that the R_{FQ} for both $\Delta\lambda$ = 15 nm and $\Delta\lambda$ = 60 nm in the presence of DPZ under any ultrasonic irradiation time are higher than the corresponding those in the absence of DPZ, which indicates that the synergistic effects of ultrasound and DPZ induce more serious damage to BSA molecules.

Three-Dimensional Fluorescence Spectra of BSA and BSA-DPZ Mixed Solutions With and Without Under Ultrasonic Irradiation

Three-dimensional fluorescence spectroscopy is a new analytical technique which is applied to investigate the conformational changes of proteins in recent years [43, 44]. The excitation wavelength, the emission wavelength and the fluorescence intensity can be used as the axes making the investigation of the characteristic conformational changes of proteins more scientific and credible [45, 46]. The three-dimensional fluorescence and contour spectra of BSA and BSA-DPZ mixed solutions under with or without ultrasonic irradiation are shown in Figs. 11 and 12, respectively, and the corresponding characteristic parameters are listed in Table 2. As shown in Figs. 11 and 12, peak 1 ($\lambda_{ex} = \lambda_{em}$) is the Rayleigh scattering peak, peak 2 ($\lambda_{em} = 2\lambda_{ex}$) is the second-order scattering peak. Peak *a* (λ_{ex} = 285.0 nm, λ_{em} = 350.5 nm) is the fluorescence peak and mainly enunciates the spectral behavior of tyrosine and tryptophan residues. Peak *b* (λ_{ex} = 285.0 nm, λ_{em} = 666.0 nm) is the second-order fluorescence peak, which is mainly caused by the transition of $\pi \rightarrow \pi^*$ of characteristic polypeptide backbone structure C = O of BSA [47]. It is

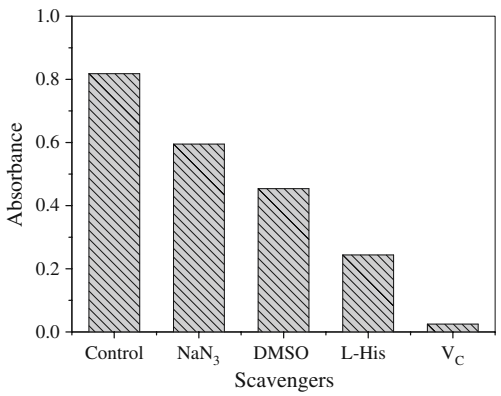

Fig. 13 Absorbance of DPCO at 563 nm in DPCI-DPZ mixed solutions in the presence of various scavengers under ultrasonic irradiation, [DPCI] = 5.00×10^{-3} mol L^{-1}, [DPZ] = 2.00×10^{-4} mol L^{-1}, [NaN_3] = [DMSO] = [L-His] = [V_C] = 5.00×10^{-2} mol L^{-1}, t_{US} = 6.0 h

obvious that both fluorescence peak *a* and *b* of BSA are quenched at different conditions, but to different extent as shown in Table 2, which indicate that their conformation have changed. Moreover, the fluorescence intensities of BSA-DPZ mixed solution under ultrasonic irradiation decrease more strikingly, which indicate that the synergistic effects of ultrasound and DPZ induce more serious damage to BSA molecules. These results coincide with those obtained from the synchronous fluorescence spectra above.

Effect of Scavengers of ROS

In this study, it can be found that the synergistic effects of ultrasound and DPZ cause an obvious increase of ROS generation, which indicates that the damage in the SDT process is related to the generation of ROS. To confirm the kinds of ROS, we tested the scavenge effect of different ROS scavengers on SDT-induced ROS generation. It is well known that NaN_3 is the scavenger of $^1O_2$ [48], DMSO is the scavenger of ·OH [49], L-His is the scavenger of $^1O_2$ and ·OH [50], and V_C can scavenge all kinds of ROS [51]. If the absorbance of DPCO at 563 nm decreases after adding some kind of scavenger, it will demonstrate there is a kind of corresponding ROS in the system. As shown in Fig. 13, the absorbance of DPCO at 563 nm decrease remarkably in the presence of V_C, which suggests that the effect of SDT on BSA damage could be mainly due to the generation of ROS. Moreover, the absorbance of DPCO at 563 nm decrease to different extent in the presence of NaN_3, DMSO and L-His, which suggests that both $^1O_2$ and ·OH are the important mediators of the damage in the SDT process.

Conclusions

The damage to BSA molecules under ultrasonic irradiation in the presence of DPZ was studied by means of absorption and fluorescence spectra. The results indicated that the synergistic effects of ultrasound and DPZ could induce the damage of BSA molecules. The damage degree of BSA molecules increased with the increase of ultrasonic irradiation time and DPZ concentration because of the increased quantities of ROS generation. The results of synchronous fluorescence and three-dimensional fluorescence spectra confirmed that the synergistic effects of ultrasound and DPZ induced the damage of BSA molecules. The mechanism of synergistic effects of ultrasound and DPZ was investigated by means of oxidation-extraction photometry combined with several ROS scavengers. The results indicated that the damage of BSA molecules could be mainly due to the generation of ROS, in which both $^1O_2$ and ·OH were the important mediators of the ultrasound-inducing damage in the presence of DPZ.

References

1. Sibata CH, Colussi VC, Oleinick NL, Kinsella TJ (2001) Photodynamic therapy in oncology. Expert Opin Pharmacother 2 (6):917–927
2. Dennis EJGJD, Dai F, Rakesh KJ (2003) Photodynamic therapy for cancer. Nat Rev Cancer 3(5):380–387
3. Kübler AC (2005) Photodynamic therapy. Med Laser Appl 20 (1):37–45
4. Usuda J, Tsutsui H, Honda H, Ichinose S, Ishizumi T, Hirata T, Inoue T, Ohtani K, Maehara S, Imai K, Tsunoda Y, Kubota M, Ikeda N, Furukawa K, Okunaka T, Kato H (2007) Photodynamic therapy for lung cancers based on novel photodynamic diagnosis using talaporfin sodium (NPe6) and autofluorescence bronchoscopy. Lung Cancer 58 (3):317–323
5. Filonenko EV, Sokolov VV, Chissov VI, Lukyanets EA, Vorozhtsov GN (2008) Photodynamic therapy of early esophageal cancer. Photodiag Photodyn Ther 5(3):187–190
6. Allison RR, Sheng C, Cuenca R, Bagnato VS, Austerlitz C, Sibata CH (2010) Photodynamic therapy for anal cancer. Photodiag Photodyn Ther 7(2):115–119
7. Chan HH, Nishioka NS, Mino M, Lauwers GY, Puricelli WP, Collier KN, Brugge WR (2004) EUS-guided photodynamic therapy of the pancreas: a pilot study. Gastrointest Endosc 59 (1):95–99
8. Allison RR, Sibata C, Mang TS, Bagnato VS, Downie GH, Hu XH, Cuenca R (2004) Photodynamic therapy for chest wall recurrence from breast cancer. Photodiag Photodyn Ther 1 (2):157–171
9. Roberts DJH, Cairnduff F (1995) Photodynamic therapy of primary skin cancer: a review. Brit J Plast Surg 48(6):360–370
10. Hachimine K, Shibaguchi H, Kuroki M, Yamada H, Kinugasa T, Nakae Y, Asano R, Sakata I, Yamashita Y, Shirakusa T, Kuroki M (2007) Sonodynamic therapy of cancer using a novel porphyrin derivative, DCPH-P-Na(I), which is devoid of photosensitivity. Cancer Sci 98(6):916–920
11. Umemura S, Yumita N, Nishigaki R, Umemura K (1990) Mechanism of cell damage by ultrasound in combination with hematoporphyrin. Jpn J Cancer Res 81(9):962–966
12. Umemura S, Yumita N, Nishigaki R (1993) Enhancement of ultrasonically induced cell damage by a gallium-porphyrin complex, ATX-70. Jpn J Cancer Res 84(5):582–588
13. Umemura S, Yumita N, Okano Y, Kaneuchi M, Magario N, Ishizaki M, Shimizu K, Sano Y, Umemura K, Nishigaki R (1997) Sonodynamically-induced in vitro cell damage enhanced by adriamycin. Cancer Lett 121(2):195–201
14. Yumita N, Sasaki K, Umemura S, Yukawa A, Nishigaki R (1997) Sonodynamically induced antitumor effect of gallium-porphyrin complex by focused ultrasound on experimental kidney tumor. Cancer Lett 112(1):79–86
15. Barati AH, Mokhtari-Dizaji M, Mozdarani H, Bathaie Z, Hassan ZM (2007) Effect of exposure parameters on cavitation induced by low-level dual-frequency ultrasound. Ultrason Sonochem 14 (6):783–789
16. Rosenthal I, Sostaric JZ, Riesz P (2004) Sonodynamic therapy-a review of the synergistic effects of drugs and ultrasound. Ultrason Sonochem 11(6):349–363

17. Liu B, Guo Y, Wang J, Xu R, Wang X, Wang D, Zhang LQ, Xu YN (2010) Spectroscopic studies on the interaction and sonodynamic damage of neutral red (NR) to bovine serum albumin (BSA). J Lumin 130(6):1036–1043
18. Zhang HX, Huang X, Zhang M (2008) Thermodynamic studies on the interaction of dioxopromethazine to β-cyclodextrin and bovine serum albumin. J Fluoresc 18(3–4):753–760
19. Li YH, Wang CY, Sun JY, Zhou YC, You TY, Wang EK, Fung YS (2005) Determination of dioxopromethazine hydrochloride by capillary electrophoresis with electrochemiluminescence detection. Anal Chim Acta 550(1–2):40–46
20. Wainwright M (2005) The development of phenothiazinium photosensitisers. Photodiagn Photodyn Ther 2(4):263–272
21. Wainwright M, Crossley KB (2004) Photosensitising agents—circumventing resistance and breaking down biofilms: a review. Int Biodeterior Biodegrad 53(2):119–126
22. Wainwright M, Mohr H, Walker WH (2007) Phenothiazinium derivatives for pathogen inactivation in blood products. J Photochem Photobiol B 86(1):45–58
23. Yumita N, Umemura S (2003) Sonodynamic therapy with photofrin II on AH130 solid tumor. Pharmacokinetics, tissue distribution and sonodynamic antitumoral efficacy of photofrin II. Cancer Chemother Pharmacol 51(2):174–178
24. Wang J, Liu LJ, Liu B, Guo Y, Zhang YY, Xu R, Wang SX, Zhang XD (2010) Spectroscopic study on interaction of bovine serum albumin with sodium magnesium chlorophyllin and its sonodynamic damage under ultrasonic irradiation. Spectrochim Acta A 75(1):366–374
25. Sasaki K, Yumita N, Nishigaki R, Sakata I, Nakajima S, Umemura S (2001) Pharmacokinetic study of a gallium-porphyrin photo- and sono-sensitizer, ATX-70, in tumor-bearing mice. Jpn J Cancer Res 92(9):989–995
26. Liu CH, Wang CH, Xu ZL, Wang Y (2007) Isolation, chemical characterization and antioxidant activities of two polysaccharides from the gel and the skin of aloe barbadensis miller irrigated with sea water. Process Biochem 42(6):961–970
27. Yumita N, Sakata I, Nakajima S, Umemura S (2003) Ultrasonically induced cell damage and active oxygen generation by 4-formyloximeetylidene-3-hydroxyl-2-vinyl-deuterio-porphynyl (IX)-6-7-diaspartic acid: on the mechanism of sonodynamic activation, BBA-Gen. Subjects 1620(1–3):179–184
28. Dai SC, Hu SS, Wu CJ (2009) Apoptotic effect of sonodynamic therapy mediated by hematoporphyrin monomethyl ether on C6 glioma cells in vitro. Acta Neurochir 151(12):1655–1661
29. Li JH, Song DY, Xu YG, Huang Z, Yue W (2008) In vitro study of haematoporphyrin monomethyl ether-mediated sonodynamic effects on C6 glioma cells. Neurol Sci 29(4):229–235
30. Feril LB Jr, Tsuda Y, Kondo T, Zhao QL, Ogawa R, Cui ZG, Tsukada K, Riesz P (2004) Ultrasound-induced killing of monocytic U937 cells enhanced by 2, 2′-azobis(2-amidinopropane) dihydrochloride. Cancer Sci 95(2):181–185
31. Miyoshi N, Tuziuti T, Yasui K, Iida Y, Shimizu N, Riesz P, Sostaric JZ (2008) Ultrasound-induced cytolysis of cancer cells is enhanced in the presence of micron-sized alumina particles. Ultrason Sonochem 15(5):881–890
32. Tang W, Liu QH, Wang XB, Wang P, Zhang J, Cao B (2009) Potential mechanism in sonodynamic therapy and focused ultrasound induced apoptosis in sarcoma 180 cells in vitro. Ultrasonics 49(8):786–793
33. Liu B, Wang J, Wang X, Liu BM, Kong YM, Wang D, Xu SK (2010) Spectrometric studies on the sonodynamic damage of protein in the presence of levofloxacin. J Fluoresc 20(5):985–992
34. Yumita N, Kawabata K, Sasaki K, Umemura S (2002) Sonodynamic effect of erythrosin B on sarcoma 180 cells in vitro. Ultrason Sonochem 9(5):259–265
35. Yumita N, Han QS, Kitazumi I, Umemura S (2008) Sonodynamically-induced apoptosis, necrosis, and active oxygen generation by mono-l-aspartyl chlorin e6. Cancer Sci 99(1):166–172
36. He LL, Wang X, Liu B, Wang J, Sun YG (2010) Interaction between ranitidine hydrochloride and bovine serum albumin in aqueous solution. J Solution Chem 39(5):654–664
37. Wang J, Zhang YY, Guo Y, Zhang L, Xu R, Xing ZQ, Wang SX, Zhang XD (2009) Interaction of bovine serum albumin with acridine orange (C.I. basic orange 14) and its sonodynamic damage under ultrasonic irradiation. Dyes Pigm 80 (2):271–278
38. Wang J, Guo YW, Liu B, Jin XD, Liu LJ, Xu R, Kong YM, Wang BX (2011) Detection and analysis of reactive oxygen species (ROS) generated by nano-sized TiO_2 powder under ultrasonic irradiation and application in sonocatalytic degradation of organic dyes. Ultrason Sonochem 18(1):177–183
39. Kardos N, Luche JL (2001) Sonochemistry of carbohydrate compounds. Carbohydr Res 332(2):115–131
40. Lakowicz JR (2006) Principles of fluorescence spectroscopy, 3rd edn. Springer Science + Business Media, New York, p 529
41. Wang CX, Yan FF, Zhang YX, Ye L (2007) Spectroscopic investigation of the interaction between rifabutin and bovine serum albumin. J Photochem Photobiol A 192(1):23–28
42. Wen MG, Zhang XB, Tian JN, Ni SH, Bian HD, Huang YL, Liang H (2009) Binding interaction of xanthoxylin with bovine serum albumin. J Solution Chem 38(4):391–401
43. Zhang HM, Wang YQ, Jiang ML (2009) A fluorimetric study of the interaction of C.I. Solvent red 24 with haemoglobin. Dyes Pigm 82(2):156–163
44. Ding F, Han BY, Liu W, Zhang L, Sun Y (2010) Interaction of imidacloprid with hemoglobin by fluorescence and circular dichroism. J Fluoresc 20(3):753–762
45. Zhang HM, Zhou QH, Wang YQ (2010) Studies on the interactions of 2, 4-dinitrophenol and 2, 4-dichlorphenol with trypsin. J Fluoresc 20(2):507–516
46. Ding F, Liu W, Zhang X, Wu LJ, Zhang L, Sun Y (2010) Identification of pyrazosulfuron-ethyl binding affinity and binding site subdomain IIA in human serum albumin by spectroscopic methods. Spectrochim Acta A 75(3):1088–1094
47. Zhang YZ, Zhou B, Zhang XP, Huang P, Li CH, Liu Y (2009) Interaction of malachite green with bovine serum albumin: determination of the binding mechanism and binding site by spectroscopic methods. J Hazard Mater 163(2–3):1345–1352
48. Bose B, Dube A (2006) Interaction of Chlorin p6 with bovine serum albumin and photodynamic oxidation of protein. J Photochem Photobiol B 85(1):49–55
49. Panganamala RV, Sharma HM, Heikkila RE, Geer JC, Cornwell DG (1976) Role of hydroxyl radical scavengers dimethyl sulfoxide, alcohols and methional in the inhibition of prostaglandin biosynthesis. Prostag 11(4):599–607
50. Yumita N, Nishigaki R, Sakata I, Nakajima S, Umemura S (2000) Sonodynamically induced antitumor effect of 4-formyloximethylidene-3-hydroxy-2-vinyl-deuterio-porphynyl (IX)-6, 7-diaspartic acid (ATX-S10). Jpn J Cancer Res 91 (2):255–260
51. Yu TH, Bai J, Hu K, Wang ZB (2003) The effect of free radical scavenger and antioxidant on the increase in intracellular adriamycin accumulation induced by ultrasound. Ultrason Sonochem 10(1):33–35